Journal of Energy and Power Engineering 18 (2024) 18-28
doi: 10.17265/1934-8975/2024.01.003

# Matlab-Simulink Simulation Model of Electric Multiple Unit (EMU) Series ŽS 413/417 in Traction and Electric Braking Mode

Branislav Gavrilovic
*Academy of Technical and Art Applied Studies Belgrade, Railway College Belgrade, Serbia*

**Abstract:** In the paper, the Matlab-Simulink model of simulation of operation of the ŽS 413/417 series EMU (electric multiple unit) in traction and braking mode is exposed where changes are observed: stator currents of three-phase traction motors, traction electric motor speeds and EMU, electromagnetic torque on the rotor shaft of the traction electric motor and DC (direct current) bus voltage. The model allowed review of the listed parameters for: different allowed values of contact network voltage and total voltage distortion at the place of connection of the EMU to the contact network, different mechanical loads of EMU and traction electric motor and different train speeds and rotation of traction electric motors. Appropriate conclusions were made through the analysis of the simulation results obtained.

**Key words:** Simulations, EMU, Serbian railways.

## 1. Introduction

The ŽS 413/417 series EMU (electric multiple unit) is a low-floor, four-part passenger train of "Serbian Railways" manufactured by the Swiss company Stadler. This light, fast innovative regional train (FLIRT: Fast Light Innovative Regional Train) is a specially designed EMU of the latest generation "FLIRT 3". At the beginning of 2014, 21 ŽS series 413/417 the electric EMUs were put into service on the electric railways of "Serbian Railways", and the procurement of thirty one more is in progress (Fig. 1) [1].

Basic technical data of the EMU of series ŽS 413/417 are shown in Table 1 [1].

The traction equipment of the EMU of the 413/417 series consists of:

- One pantograph for 25 kV AC (alternating current)
- One traction transformer
- Two power converters and four traction motors (2 traction motors per one power converter)
- Single-axle drive with three-phase asynchronous motors

The traction motor is installed in the motor bogie. Wheelset axle shaft, traction motor, tooth coupling and the gearbox together form an axle drive. There are two axle drives per motor bogie. The traction motor transmits the torque to the gearbox through the tooth coupling transmission ratio of 1:5.9714. The gearbox transmits the drive torque through the wheelset axle shaft to the wheels and the tracks [1].

Traction system of the train is shown in Fig. 2.

Fig. 3 shows the tractive force-speed characteristics of the EMU [1, 2].

Fig. 4 shows the power dependent on the line voltage of the EMU.

**Corresponding author:** Branislav Gavrilovic, PhD, professor, research field: train traction.


**Fig. 1 The EMU of series ŽS 413/417.**

**Table 1 Technical data.**

| | |
|---|---|
| Track gauge | 1,435 mm |
| Max. velocity | 160 km/h |
| Axle arrangement | Bo' 2' 2' 2' Bo' |
| Traction mode | 25 kV AC, 560 Hz |
| Maximum power on the wheel | 1,540 kW |
| Maximum starting tractive force | 160 kN |
| Traction transformer (main data) | |
| Marked power | 605 kVA |
| Maximum power per traction winding | 500 kVA |
| Nominal voltage of traction windings | Approx. 25 kV/500 V and no load |
| Traction converter-Line inverter-AFE (Active Front End) | |
| Input voltage | Approx. 500 VAC |
| Maximum input current | Approx. 1,020 per AFE (2,040 total) |
| Nominal DC-link | 950 V (under 1,000 V) |
| Maximum output power | Approx. 525 per AFE (1,050 total) |
| Bus capacity | 85 mF |
| Train wide AFE synchronization | 6 converters-3 EMU in multiple traction |
| Motor inverter (Traction three-phase inverter) | |
| Power in traction | 385 kW (at wheel) |
| Output voltage traction | 20 Hz to 120 Hz approx. from 211 V to 630V<br>120 Hz to 215.7 Hz approx. 675 V |
| Output maximum current | Approx. 780 Hz (700 Hz switching frequency) |
| Traction motor data | |
| Traction motor are three-phase asynchronous motors type | TMF 54-32-4 |
| Continuous power | 300 kW |
| Transmission ratio | 1:5.9714 |

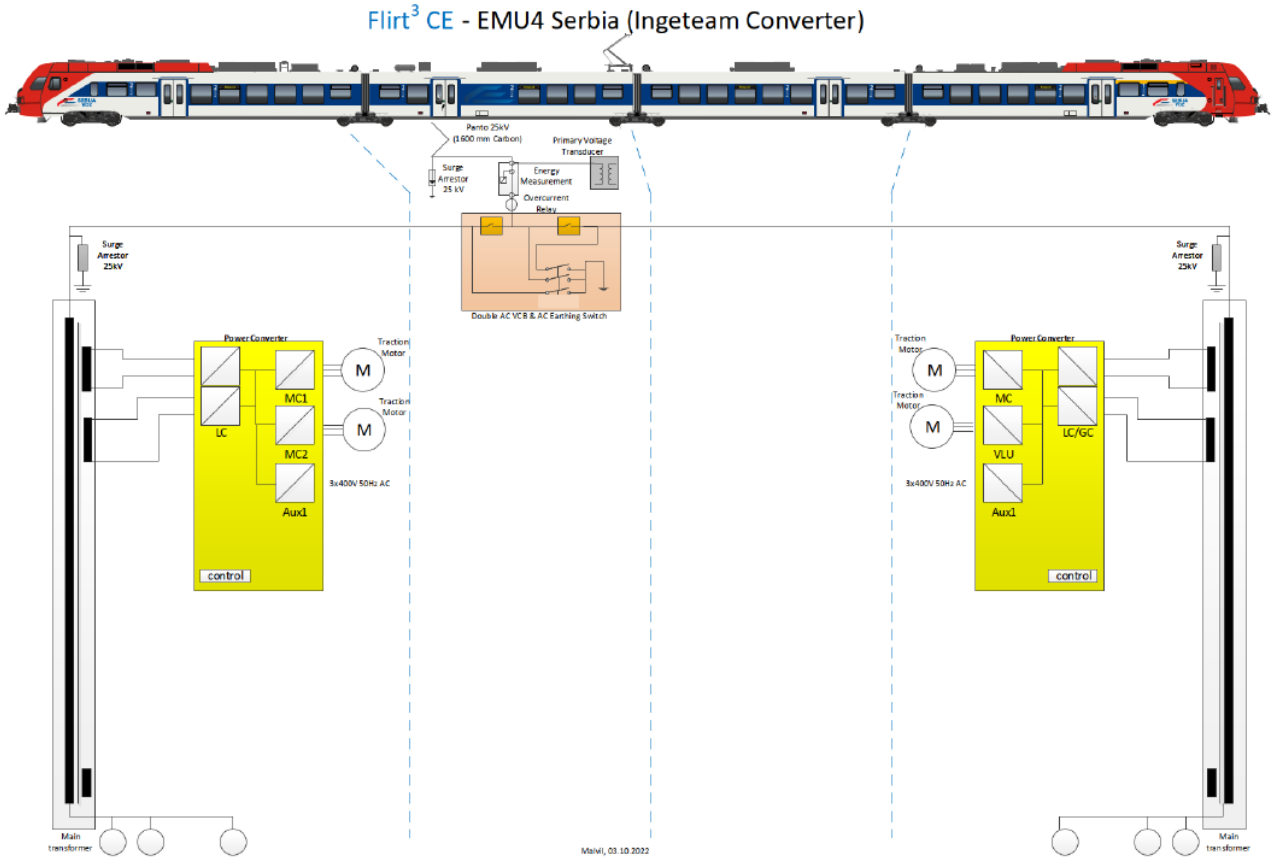


**Fig. 2 Principle circuit diagram main current of EMU.**

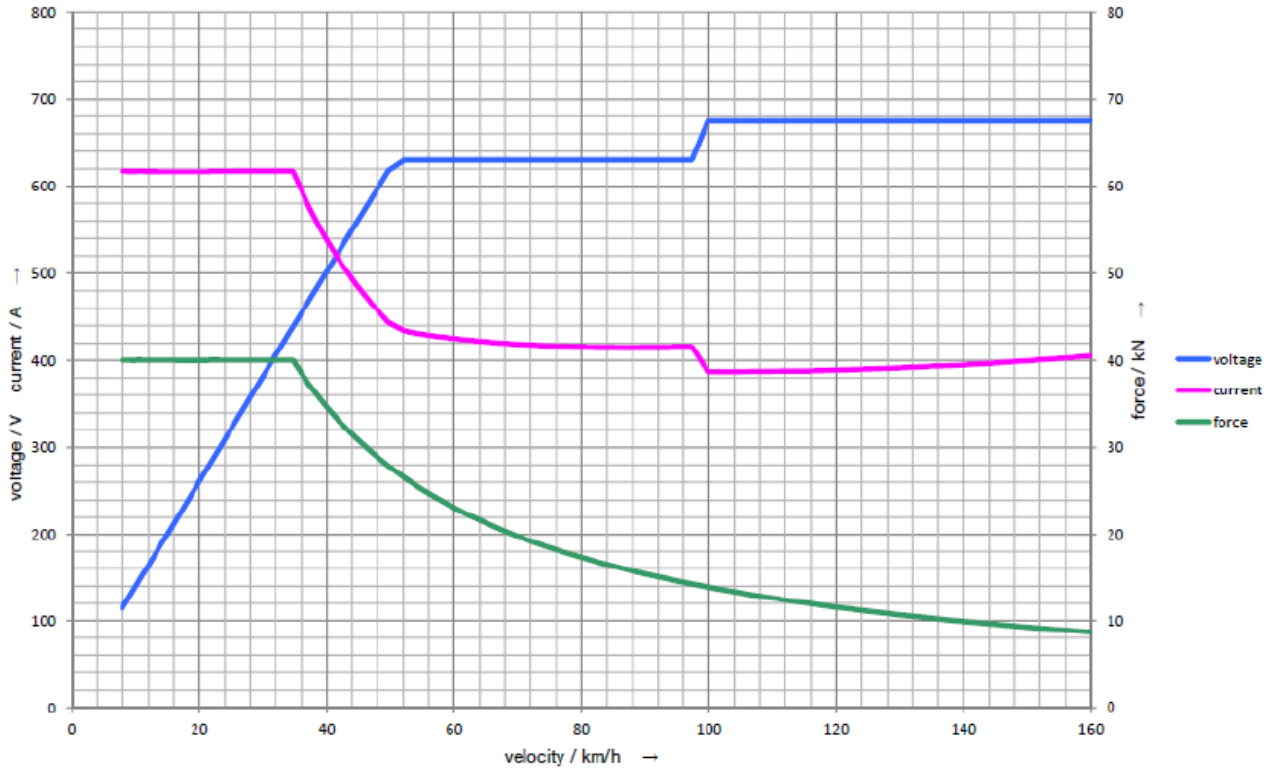


**Fig. 3 Traction force characteristic.**

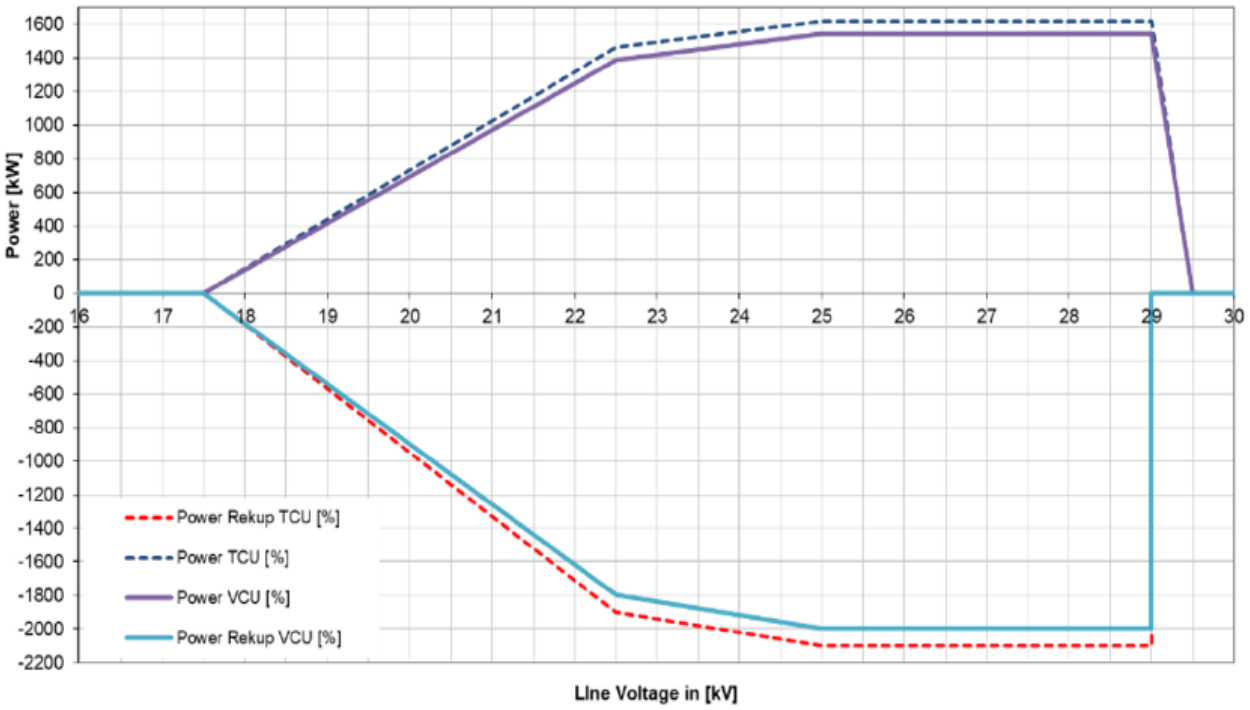


**Fig. 4 Power dependent on the line voltage.**

## 2. Modeling EMU in Matlab-Simulink

Modeling of EMU of series ŽS 413/417 shown in Matlab-Simulink is shown in Fig. 5.

The high level block of EMU series ŽS 413/417 schematic shown below is built from six main blocks (Figs. 6 and 7). The traction transformer, the induction motor, the three-phase inverter, and the mono-phase diode rectifier models are provided with the SimPowerSystems™ library. The speed controller, the braking chopper, and the DTC (direct torque and flow control) controller models are specific to the drive library.

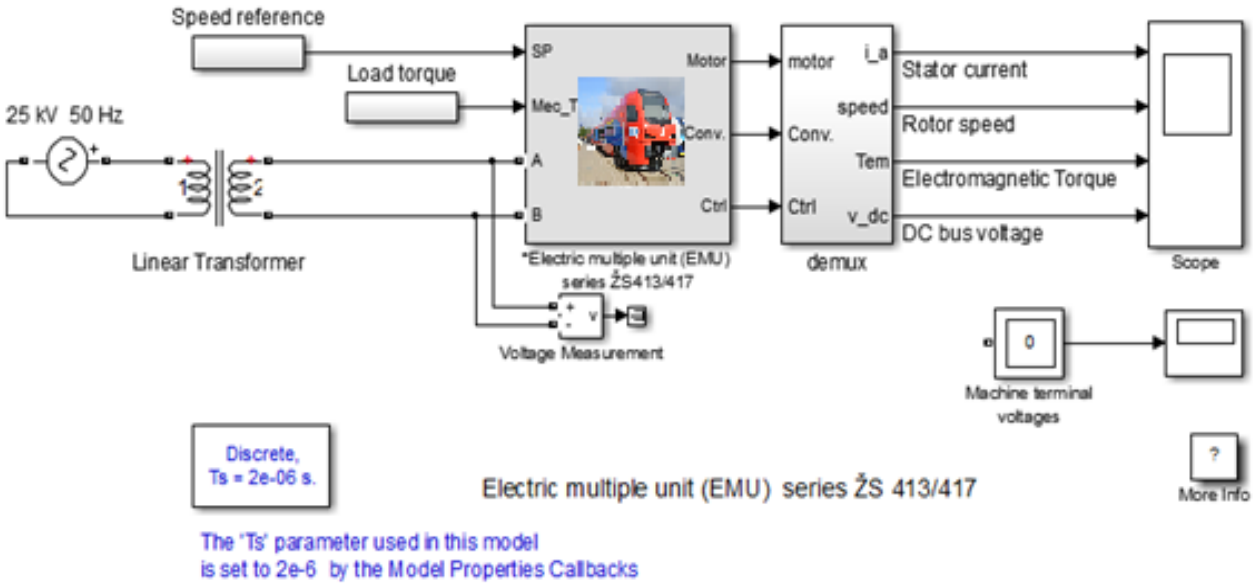


**Fig. 5 Simulink model of the EMU series ŽS 413/417.**

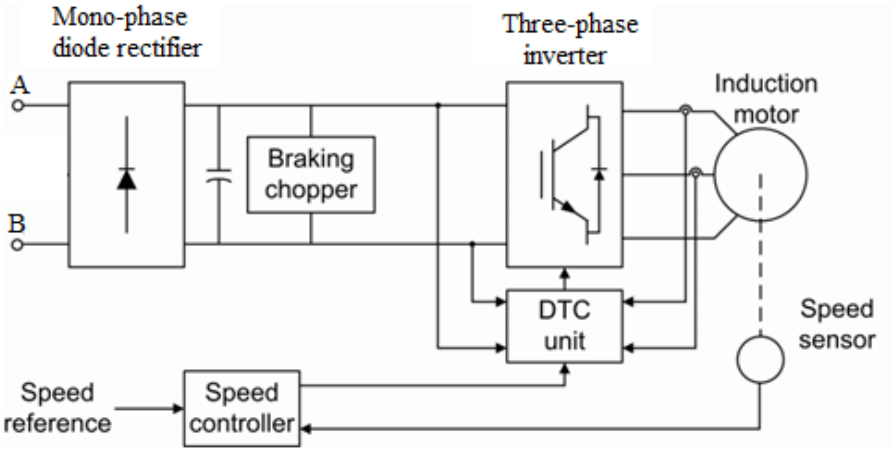


**Fig. 6 The high level block schematic of EMU series ŽS 413/417.**

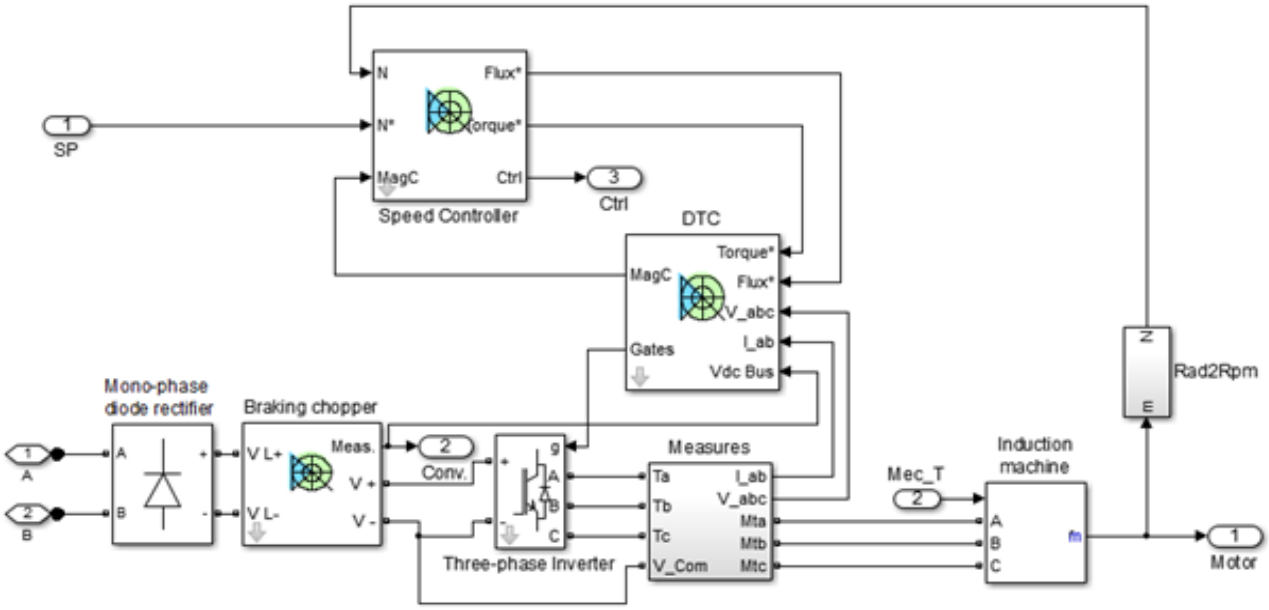


**Fig. 7 Simulink schematic of EMU series ŽS 413/417 built from six main blocks.**

*2.1 Speed Controller*

The speed controller is based on a PI (proportional-integral) regulator shown below. The output of this regulator is a torque set point applied to the DTC controller block [3-5].

The high-level block diagram as well as the Simulink model of the speed controller are shown in Figs. 8 and 9 [3-5].

*2.2 Braking Chopper*

The braking chopper block contains the DC (direct current) bus capacitor and the dynamic braking chopper, which is used to absorb the energy produced by a motor deceleration. Simulink model of Braking chopper is shown in Fig. 10 [3-5].

*2.3 DTC Controller*

The DTC controller contains five main blocks, shown in Fig. 11 [3-5].

The *torque & flux calculator* block is used to estimate the motor flux αβ components and the electromagnetic torque. This calculator is based on motor equation synthesis.

The αβ *vector* block is used to find the sector of the αβ plane in which the flux vector lies. The αβ plane is divided into six different sectors spaced by 60 degrees.

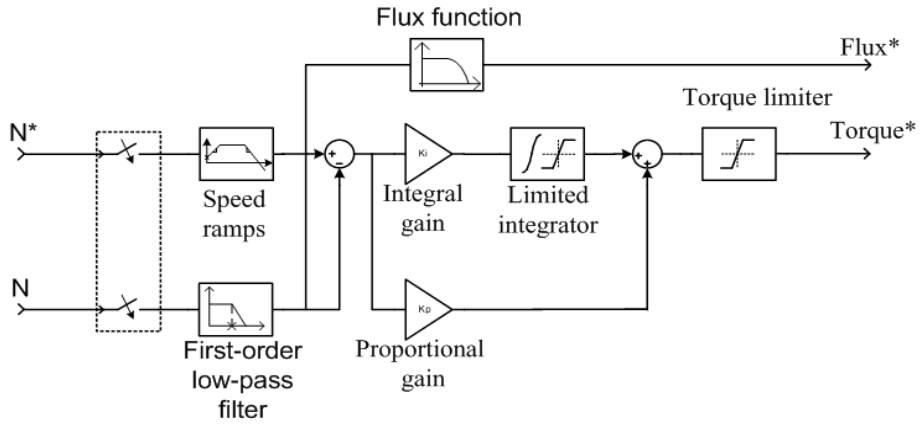


**Fig. 8 The high level block schematic of speed controller.**

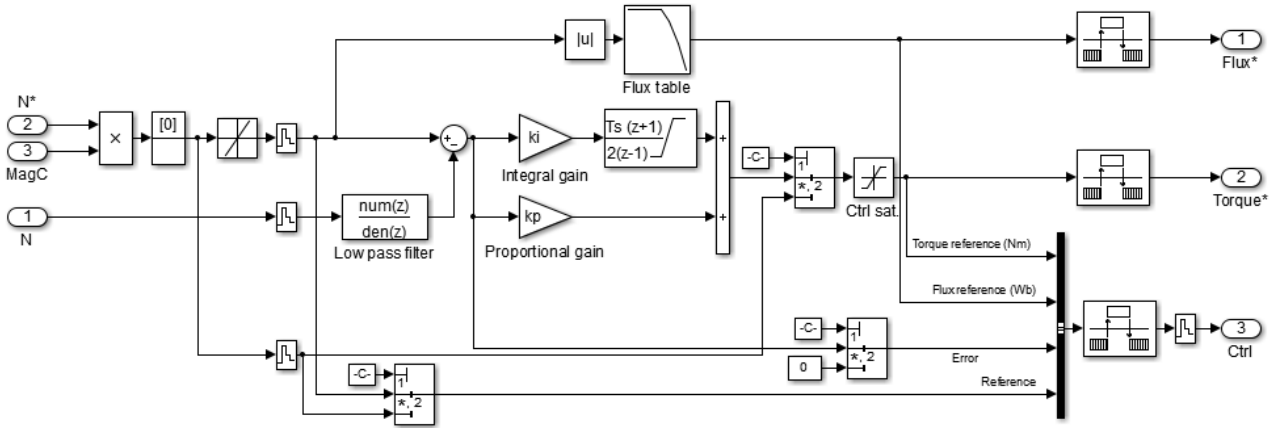


**Fig. 9 Simulink model of speed controller.**

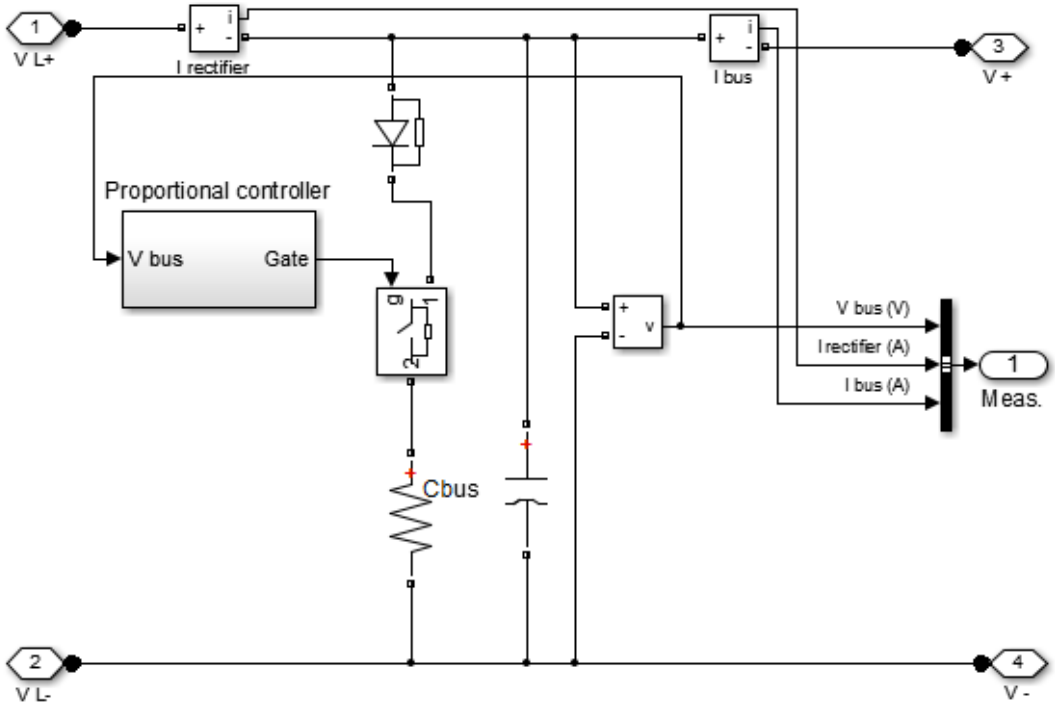


**Fig. 10 Simulink model of braking chopper.**

The *Flux & Torque Hysteresis* blocks contain a two-level hysteresis comparator for flux control and a three-level hysteresis comparator for the torque control. The description of the hysteresis comparators is available below.

The *Switching table* block contains two lookup tables that select a specific voltage vector in accordance with the output of the *Flux & Torque Hysteresis* comparators. This block also produces the initial flux in the machine.

The *Switching control* block is used to limit the inverter commutation frequency to a maximum value specified by the user.

The high-level block diagram as well as the Simulink model of direct torque and flux control of the drive induction motor are shown in Figs. 11 and 12 [3-5].

### *2.4 Measurements*

In this model, the voltage of the contact network at the connection point of the EMU series ŽS 413/417 is taken as an input variable electrical quantity. This voltage can be changed within the limits of 17.5-27.5 kV according to the provisions of EN 50163. All other parameters of the Simulink model blocks are determined by the technical data of the train's devices and equipment. Electrical quantities that are measured during dynamic processes are: the stator current of the traction electric motor and the DC bus voltage converter.

The given input mechanical parameters of the model are: the desired final speed of rotation of the rotor of the traction electric motor ($\omega_r$) and the resistive torque of the train movement ($T_m$). Mechanical quantities that are measured during dynamic processes and achieving the desired rotation speed are: the reverse electromagnetic torque of the traction electric motor ($T_e$) and the change in the rotation speed of the rotor of the traction electric motor ($\omega_r$).

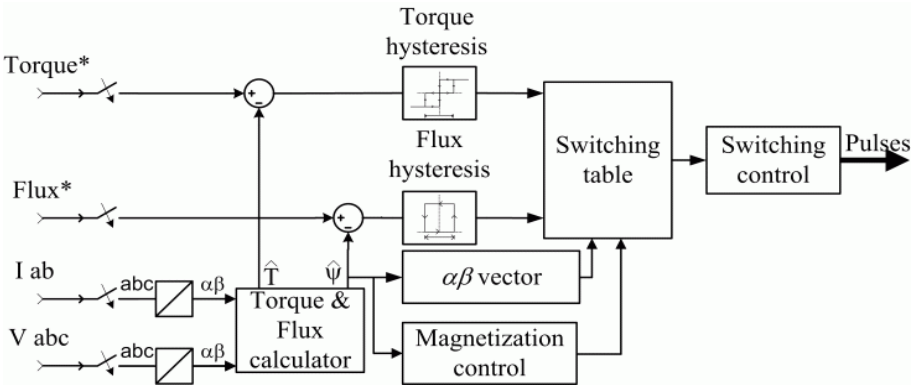


**Fig. 11 The DTC controller.**

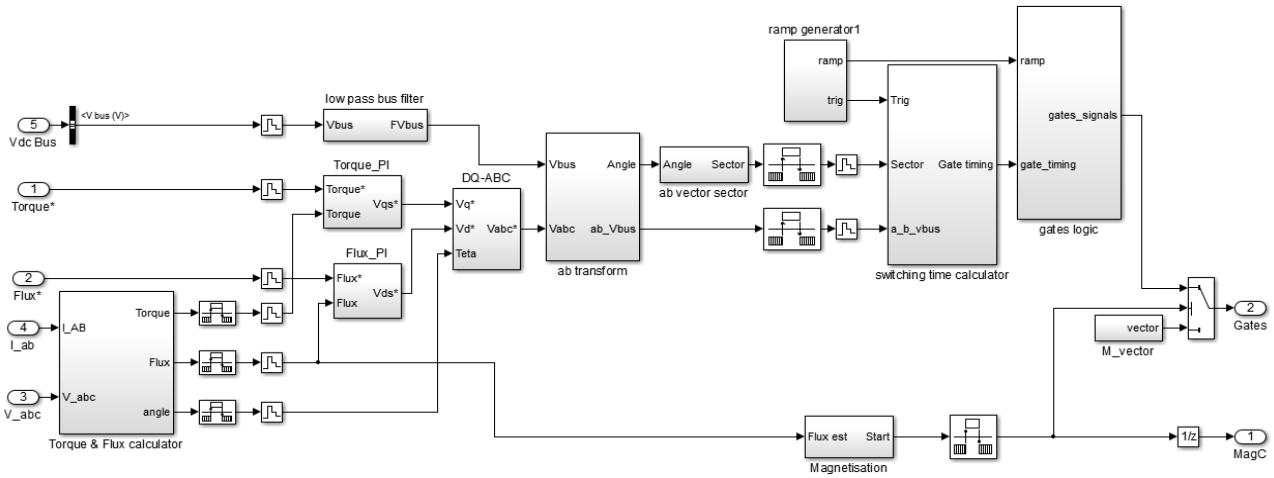


**Fig. 12 Simulink model of DTC (direct torque and flux control) of the drive induction motor.**

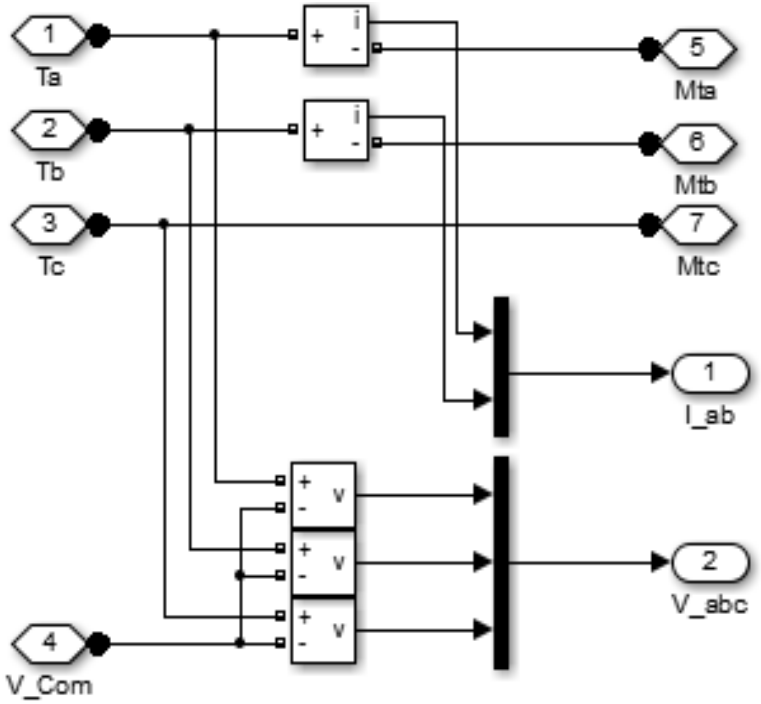


**Fig. 13 Simulink model of measures.**

When calculating the reverse electromagnetic moment on the shaft of the traction electric motor ($T_e$), the equation of the dynamic balance of the train drive train was used [6-18].

$$T_e = J\frac{d}{dt}\omega_r + F\omega_r + T_m \tag{1}$$

Wherein:

$\omega_r$—speed of rotation of the rotor of the electric motor,

$J$—the moment of inertia of all rotating masses reduced to the rotor side of the electric motor,

F—coefficient of viscous friction,

$T_m$—resistance moments of movement reduced to the rotor side of the electric motor.

By measuring and knowing the value of the reverse electromagnetic torque of the traction electric motor ($T_e$) and the change in the rotation speed of the rotor of the traction electric motor ($\omega_r$), the traction force between the wheel and the rail ($F_v$), i.e. the translational speed of the train ($v$), is fully determined. The relationship between the rotating electromagnetic torque of the traction electric motor ($T_e$) and the traction force ($F_v$), i.e. the rotation speed of the rotor of the traction electric motor ($\omega_r$) and the translation speed of the train ($v$) is given by the following equations [2]:

$$F_v = \frac{2\cdot i\cdot \eta}{D}\cdot T_e \tag{2}$$

$$v = \frac{D}{2\cdot i}\cdot \omega_r \tag{3}$$

Wherein.

$i$—transmission ratio of the reducer (5.9714),

$\eta$—degree of utilization of the reducer (0.94),

$D$—the diameter of the EMU monobloc wheel (new/worn: 760/690 mm),

In order to monitor the change in stator current, rotation speed and electromagnetic torque of the drive motor as well as DC bus voltage, a Simulink measurement block was modeled as in Fig. 13.

## 3. Results of Simulations

Assuming that the EMU:

- supplies with a stable sinusoidal voltage of 25 kV, 50 Hz,
- starts from rest at time $t$ = 0 s: up to the speed of the electric motor $\omega_r$ =1,500 rpm ($v$ = 90 km/h),
- loads it so that the resistance torque on the electric motor shaft is $T_m$ = 792 Nm in an interval of 0.5-1.5 s,

and after 1.5 s it is equal to $T_m$ = -792 Nm.

- starts braking from the moment $t$ = 1 s, and so on, the simulation results are given in Fig. 14.

The simulation results show that the acceleration of the train up to $t$ = 0.5 s is achieved with a constant electromagnetic moment on the electric motor shaft of $T_e$ = 810 Nm, and when the load on the electric motor increased, the electromagnetic moment also increased to $T_e$ = 1,050 Nm. The speed of the electric motor $\omega_r$ = 1,500 rpm ($v$ = 90 km/h) is reached at the moment $t$ = 1 s when braking starts until $t$ = 1.75 s when the EMU stops. It is interesting to note that the speed of $\omega_r$ = 1,500 rpm is not reached before $t$ = 1 s and if the limiters allow it even earlier. The rotating electromagnetic torque on the electric motor shaft is very small during braking in the interval from $t$ =1-1.5 s because the motor brakes due to the drag resistance of $T_m$ = +792 Nm, and from $t$ > 1.5 s a negative (braking) electromagnetic is generated the moment that overcomes the inertial drag resistance of $T_m$ = -792 Nm, bringing the train to rest.

With these input parameters, the stator current of the electric motor does not exceed 1,000 A, and the DC bus voltage of 800 V.

If the same input parameters of the system as in the previous example are assumed, but now with a new set speed of the electric motor of $\omega_r$ = 500 rpm ($v$ = 30 km/h), the change in the output values is shown in Fig. 15.

In this case, the starting of the electric motor from rest is done with a smaller electromagnetic moment $T_e$ = 200 Nm until the moment $t$ = 0.5 s when the electric motor is loaded with $T_m$ = 792 Nm and increases to the value $T_e$ = 810 Nm.

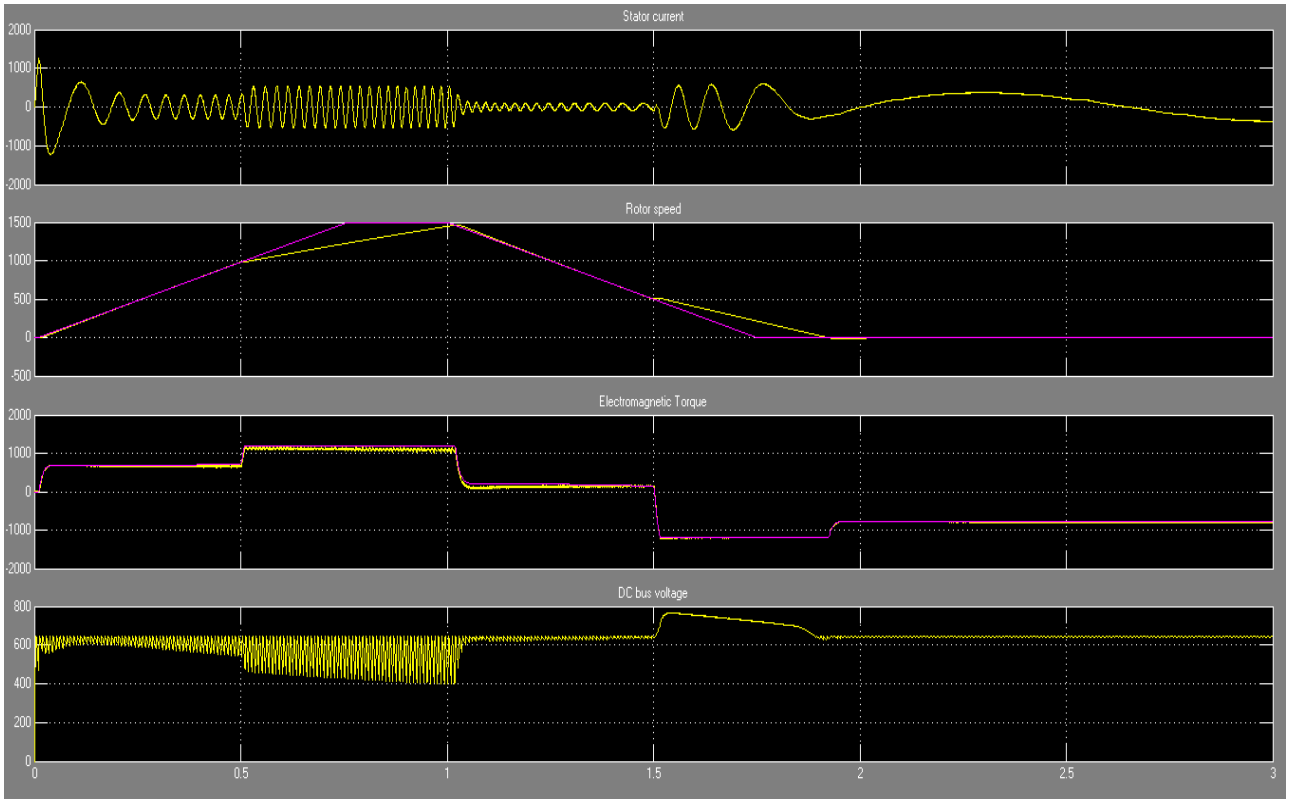


**Fig. 14 Changes in the stator current, rotation speed and electromagnetic moment of the electric motor and DC bus voltage of the DC medium of the inverter EMU for $\omega_r$ =1,500 rpm and $T_m$ = ±792 Nm.**

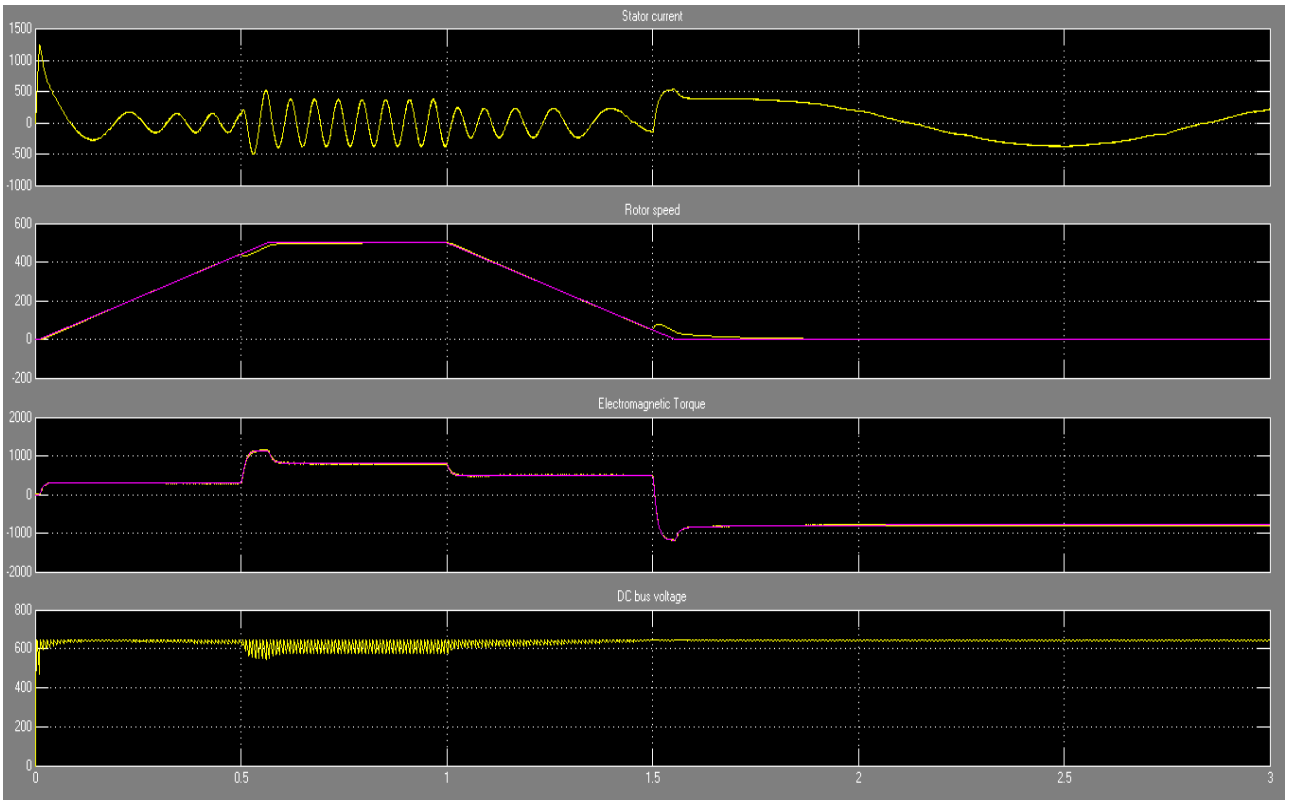


**Fig. 15 Changes in the stator current, rotation speed and electromagnetic moment of the electric motor and DC bus voltage of the DC medium of the inverter EMU for $\omega_r$ = 500 rpm and $T_m$ = ±792 Nm.**

The set speed of $\omega_r$ = 500 rpm ($v$ = 30 km/h) is reached at the moment $t$ = 0.6 s and is maintained until the moment $t$ = 1 s when the start of braking is set. Braking starts with an electromagnetic torque $T_e$ smaller than the positive resistive torque of $T_m$ = +792 Nm and lasts until a complete stop at the moment $t$ = 1.5 s. For $t$ > 1.5 s the electric motor remains braked due to the generation of a negative electromagnetic moment $T_e$ that overcomes the negative resistance of $T_m$ = -792 Nm.

With these input parameters, the stator current of the electric motor does not exceed 600 A, and the DC bus voltage of 620 V.

Numerous simulations with the specified input parameters, but now with variable and permitted contact network voltage values from 19.5 to 27.5 kV and a total voltage distortion equal to or less than 8% (EN 50162) show the same or approximately the same change in output values as in Figs. 14 and 15.

This fact indicates a very important feature of the ŽS 413/417 series EMU, which is that the train's electric traction drive has completely eliminated the influence of the contact network voltage. Due to the mentioned fact, it can be concluded that these EMUs represent a good driving railway solution.

The presented simulation results are fully confirmed with the experimental results presented in the literature [1].

Finally, it should be noted that the described Matlab-Simulink model of simulation of operation of the ŽS 413/417 series EMU in traction and braking mode enables the analysis of numerous other operating conditions that can be the subject of future research.

## 4. Conclusion

The described simulation model completely objectively depicts the operation of the EMU of the ŽS 413/417 series in traction and braking mode. The model made it possible to observe the electrical and mechanical parameters of the drive three-phase

asynchronous motors for: different permissible voltage values and voltage distortions at the point of connection of the multiple power unit to the contact network, different mechanical loads and different rotation speeds of traction electric motors.

Numerous simulations show a very important feature of the EMU of the ŽS 413/417 series, which is that the vehicle's automatic regulation system has completely eliminated the influence of changing voltage value and voltage distortion in the contact network on the vehicle's operation. This stability of the drive to changes in voltage value and voltage distortion in the contact network is very important in the exploitation of railway electric traction vehicles and represents a special quality of this EMU.

The results of the simulations were fully confirmed by the experimental measurements performed at the EMU of the ŽS 413/417 series.

## References


[1] Stadler. 2023. "Train Description—L-4547 Flirt 3 EMU Serbia." Document No. PR_5382875.

[2] Gavrilovic, B., Bundalo, Z., and Blagojevic, Z. 2019. "Regenerative Braking of Electric Multiple Unit Serie 413/417 of Joint Stock Company for Passenger Railway Transport, Serbia Voz." In *Proceedings of the 18th International Symposium INFOTEH-JAHORINA*, 20-22 March 2019.

[3] Bose, B. K. 2002. *Modern Power Electronics and AC Drives.* Englewood Cliffs: Prentice-Hall.

[4] Grelet, G., and Clerc, G. 1997. *Actionneurs électriques.* Paris: Éditions Eyrolles. (in French)

[5] Krause, P. C. 1986. *Analysis of Electric Machinery.* New York: McGraw-Hill.

[6] Branislav, G. 2023. *Research and Analysis in the Electric Traction System of the Serbian Railways*. Chisinau: Eliva Press.

[7] Boldea, I., and Nasar, S. A. 2017. *Electric Drives* (3rd ed.). Boca Raton: CRC Press.

[8] Nondahl, T. A. 1993. "Microprocessor Control of Motor Drives and Power Converters, Tutorial Course." In *Proceedings of the IEEE Industry Application Society*, October 1993, pp. 7.1-7.26.

[9] Bolton, W. M. 2004. *Electronic Control Systems in Mechanical and Electrical Engineering* (3rd ed.). London: Pearson Education.

[10] Kaur, H. 2019. *Electric Drives and Their Controlling Techniques* (1st ed.). London: Scholar's Press.

[11] Mohan, N., and raju, S. 2021. "*Analysis and Control of Electric Drives: Simulations and Laboratory Implementation*. Hoboken, NJ: John Wiley & Sons, Inc.

[12] Merabet, A. 2020. *Advanced Control Systems for Electric Drives.* Basel: MDPI.

[13] Dorji, C. 2012. "Review of Electric Motor Drives." *Machine Drives and Control*, College of Science and Technology, Department of Electrical Engineering, Royal University of Bhutan, DOI: 10.13140/RG.2.1.1198.6408. https://www.researchgate.net/publication/282291981_REVIEW_OF_ELECTRIC_MOTOR_DRIVES.

[14] Golnaraghi, F., and Kuo, B. C. 2010. *Automatic Control Systems* (9th ed.). Hoboken, NJ: John Wiley and Sons Inc.

[15] Kryukov, O. V., Blagodarov, D. A., Dulnev, N. N., and Kostin, A. A. 2018. "Intelligent Control of Electric Machine Drive Systems." In *Proceedings of the X International Conference on Electrical Power Drive Systems (ICEPDS)*, 3-6 October 2018, Novocherkassk, Russia.

[16] Hughes, A. 2006. Electric *Motors and Drives—Fundamentals: Types and Applications* (3rd ed.). Oxford, UK: Elsevier.

[17] Schröder, D. 2007. *Elektrische Antriebe—Grundlagen* (3rd ed.). Berlin, Germany: Springer-Verlag.

[18] Jauch, C., Tamilarasan, S., Bovee, K., Güvenc, L., and Rizzoni, G. 2018. "Modeling for Drivability and Drivability Improving Control of HEV." *Control Engineering Practice* 70: 50-62.